NeuroImage 81 (2013) 1–7

Contents lists available at SciVerse ScienceDirect

NeuroImage

journal homepage: www.elsevier.com/locate/ynimg

Micro-structural assessment of short term plasticity dynamics

Ido Tavor [a], Shir Hofstetter [a,b], Yaniv Assaf [a,b,*]

[a] Department of Neurobiology, Faculty of Life Sciences, Tel Aviv University, Tel Aviv, Israel
[b] Sagol School of Neuroscience, Tel Aviv University, Tel Aviv, Israel

ARTICLE INFO

Article history:
Accepted 9 May 2013
Available online 20 May 2013

Keywords:
Plasticity
Diffusion MRI
DTI
CHARMED
Short-term learning

ABSTRACT

Diffusion MRI enables the non-invasive investigation of neuroplasticity in the human brain. A recent DTI study has shown that a short learning task of only 2 h can yield changes in diffusion parameters. In the current study we aimed to discover whether a biophysical model of diffusion MRI, the CHARMED framework, which models hindered and restricted compartments within the tissue can constitute a more specific method than DTI to study structural plasticity. In addition we set to explore the time scale of the MRI learning-induced-changes. Subjects were scanned with both DTI and CHARMED before and after participating in the same car-racing task. Repetition of a shorter version of the task was done the following week. Results provide additional support to the former discovery of reduction in mean diffusivity after 2 h training using DTI. In addition we show that the CHARMED framework provides a more sensitive method than DTI for discovering microstructural modification. An increase in the fraction of the restricted compartment (Fr) was found after participating in the tasks. Between tasks values of Fr returned to baseline, reflecting the dynamics of structural remodeling. By modeling different compartments in the tissue we suggest that interpretation of the biological processes that induced changes in diffusion is more straightforward, and allows improved detection of the progression of these changes.

Introduction

Neuroplasticity is the ability of the nervous system to reorganize and adapt in reaction to internal or external stimuli. Such modifications occur during development, in the process of rehabilitation after brain injuries, and as a result of life experiences (*i.e.* learning and memory) (Galván, 2010; Johnston, 2009; Maguire et al., 2000). Plasticity is observed in a variety of levels, ranging from molecular changes in synapses and cell compartments (neurons or glia), remodeling of neuronal networks, to modifications at the gross anatomy level (Bruel-Jungerman et al., 2007a, 2007b; Holtmaat and Svoboda, 2009).

Magnetic resonance imaging (MRI) enables the investigation of the living brain non-invasively, both in humans and in animal models. Characterizing structural brain plasticity with MRI has gained a lot of interest in recent years. The first studies in this field found differences in brain volume between experts and non-experts at specific domains (Maguire et al., 2000; Münte et al., 2002). The dissimilarities between these groups are believed to originate from different life experience and are thought to be evidence of gross anatomy neuroplasticity. Other studies found that structural changes can also arise following a few months of learning and training of a newly acquired skill (Bezzola et al., 2011; Draganski et al., 2004; Scholz et al., 2009).

In a previous work we explored the ability of diffusion tensor imaging (DTI), a diffusion MRI framework, to detect microstructural changes after performing a short spatial navigation task (Sagi et al., 2012). Subjects were scanned with DTI before and after a learning task of 2 h, which was based on a computer car racing game (Electronic Arts©). The main result of this study showed a significant mean diffusivity (MD) decrease in the hippocampus and para-hippocampal gyrus, suggesting a more dynamic timescale of neuroplasticity.

DTI is regarded as a micro-structural probe (Assaf and Pasternak, 2008; Basser, 1995), and as such provides a powerful method to investigate structural neuroplasticity. Although presenting new and important insights on tissue microstructure, the measured tensor in the DTI model is an average of all cellular compartments within the measured voxel and is therefore less accurate in describing the underlying tissue and its elemental compartments (Assaf et al., 2004).

Several models have been suggested to allow a more comprehensive model of diffusion in the tissue than the diffusion tensor (Alexander et al., 2010; Barazany et al., 2009; Tuch et al., 2002). The composite hindered and restricted model of diffusion (CHARMED) was proposed by Assaf et al. (2004). While DTI is a mathematical model, CHARMED is a biophysical model that refers to the different compartments of the tissue and to the specific geometry of each compartment, and this is its greatest strength. The model requires the acquisition of both high and low b value images in different gradient directions and separates the signal decay into hindered (extra-cellular water) and restricted (intracellular water) compartments (Assaf et al., 2004). The CHARMED framework can provide several parameters, one of them is the volume

* Corresponding author at: Department of Neurobiology, Faculty of Life Sciences, Tel Aviv University, Ramat Aviv, Tel Aviv 69978, Israel. Fax: +972 3 6407168.
E-mail address: assafyan@post.tau.ac.il (Y. Assaf).

1053-8119/$ – see front matter © 2013 Elsevier Inc. All rights reserved.
http://dx.doi.org/10.1016/j.neuroimage.2013.05.050

fraction of the restricted compartment (Fr), which was used in the current study (Assaf and Basser, 2005).

By modeling the brain tissue as a summation of two processes, the CHARMED framework provides the opportunity to look for the origin of the MD decrease observed in the previous study by Sagi et al. In the present study we wished to examine whether CHARMED can constitute a more specific method than DTI to study structural plasticity. For that purpose we used the same car-racing task, and scanned a new cohort of subjects with CHARMED as an additional sequence to DTI before and immediately after the task. In addition, we set to explore the time scale of the MRI learning-induced-changes. To do so, a second training episode took place a week after the first learning experience. Again, subjects were scanned with CHARMED and DTI before and immediately after the task.

Material and methods

Subjects

The study participants were 23 healthy adult volunteers (9 males and 14 females, all right-handed). The age range was 21–38 (mean 26.6; S.D. 4.2). The research protocol was approved by the Institutional Review Board of the Tel Aviv Sourasky Medical Center and all participants signed an informed consent form. None of the subjects had a history of neurological disease, psychological disorders, drug or alcohol abuse, or use of neuropsychiatric medication. All had intact vision.

Learning task

The task was based on a computer car racing game (the Need for Speed, Electronic Arts©), consisting of 16 laps (trials) of the same car game track, divided into four sessions (see Sagi et al., 2012). The objective was to learn the track and achieve better lap times. To enhance memorization, at the end of each session subjects were given snapshots of locations in the track and were required to arrange them in the correct order. In addition, they were asked to sketch an outline of the track at the end of each session. On average, subjects were engaged in the task for 90 min.

A second training episode took place 6–8 days after the first learning experience. 14 subjects (mean age 26.9, S.D. 4.4; 6 males and 8 females) returned the following week and completed a shorter training session that included 8 trials (divided into two sessions) and lasted for approximately 45 min.

MRI acquisition

Magnetic resonance imaging (MRI) was performed at the Tel Aviv Sourasky Medical Center with a 3 T (GE, Milwaukee, USA) MRI system. All subjects underwent a series of scans before and after each learning episode. At the first learning session the scans were taken approximately 2 h apart. The following week scans were taken about 1 h apart as the learning session was shorter.

The MRI protocol included DTI acquisition after each session. The first series of scans also included conventional anatomic sequences for radiological screening. In addition, the group of 14 subjects that returned for a second training session included additional acquisition of DTI and CHARMED. For this cohort, CHARMED was acquired in all scans (before and after each learning session). All MRI scans were acquired with an 8-channel head-coil. We started each series of scans with conventional anatomical sequences, then the CHARMED protocol was acquired, and finally DTI was acquired last. The CHARMED and DTI acquisition (described below) were adjusted to achieve similar SNR (in the b0) and similar acquisition time to allow comparison between methods.

Conventional anatomic sequences

T1 weighted images were acquired with a 3D spoiled gradient-recalled echo (SPGR) sequence with the following parameters: up to 160 axial slices (whole brain coverage), TR/TE = 9/3 ms, resolution $1 \times 1 \times 1$ mm^3, and scan time 4 min. In addition to the T1 scan, T2 weighted images (TR/TE = 6500/85) and FLAIR images (TR/TE/TI = 9000/140/2100) were obtained. The entire anatomical data set was used for radiological screening.

DTI protocol

Double refocused spin-echo diffusion weighted echo-planar imaging sequences were performed with up to 70 axial slices (to cover the whole brain) and image resolution of $2.1 \times 2.1 \times 2.1$ mm^3, reconstructed to $1.58 \times 1.58 \times 2.1$ mm^3 (field of view was 202 mm^2 and acquisition matrix dimension was 96×96 reconstructed to 128×128). Diffusion parameters were: $\Delta/\delta = 33/26$ ms, b value of 1000 s/mm^2 was acquired with 19 gradient directions and an additional image was obtained with no diffusion weighting (b0 image). The double-refocused sequence was used in order to minimize eddy currents. The DTI scan was repeated three times to increase signal-to-noise ratio. The total acquisition time of the DTI scans was 17 min.

CHARMED protocol

Double refocused spin-echo diffusion weighted echo-planar imaging sequences were performed with up to 40 axial slices (to cover the whole brain) and resolution of $2.4 \times 2.4 \times 3.0$ mm^3 reconstructed to $1.5 \times 1.5 \times 3.0$ mm^3 (field of view was 192 mm^2 and acquisition matrix dimension was 80×80 reconstructed to 128×128). Diffusion parameters were: $\Delta/\delta = 39/32$ ms; 34 diffusion weighted images in different gradient directions and increasing b values (208, 2250 and 4000) were acquired. The number of excitations (NEX) was 2. Total acquisition time was approximately 18 min.

Data analysis

Correction of head motion image artifacts, registration and normalization were performed using the SPM software (UCL, London, UK).

DTI analysis

First, DW images were corrected for motion using a least-squares algorithm and 6-parameter (rigid-body) transformations. Then, we performed DTI analysis using the DiVa software implemented in MATLAB 7.11.0 (Mathworks, Natick, MA), from which maps of fractional anisotropy (FA) and mean diffusivity (MD) were computed.

CHARMED analysis

The high b value images were corrected for motion using the UNDISTORT method (Ben-Amitay et al., 2012). Then, we performed CHARMED analysis using an in-house software (Assaf and Basser, 2005), from which maps of the volume fraction of the restricted compartment were computed (Fr).

Image processing

The Fr maps were co-registered to the DTI images (according to the b0 images), and then normalization procedures were done on all DTI and CHARMED images together. Optimized spatial normalization was applied utilizing the FA maps to ensure optimal alignment for voxel-based statistics. The procedure included the following steps:

a. FA template creation: A single-subject b0 image was normalized to the Montreal Neurological Institute template using a 12-parameter affine transformation followed by non-linear transformations. The same transformations were then applied on the subject's FA map.
b. Creation of an average FA map for each subject: Since subjects were scanned pre and post each learning episode, each had 4 FA maps (before and after a task). To create an average map, all FA maps

were skull-stripped and co-registered to the template. An average map for each subject was then calculated.

c. Normalization: All maps were normalized twice. First, all FA maps of each subject were normalized to his/her own average FA map using a 12-parameter affine transformation followed by nonlinear transformations. The same transformations were then applied to the MD and Fr maps. Second, all FA maps were normalized to the template as above, and transformations were then applied to the MD and Fr maps. Both normalization procedures included smoothing of 2-mm Gaussian kernels of the source image.

After normalization, we performed spatial smoothing with 8-mm FWHM Gaussian kernels on all images.

Statistical analysis

Voxel-based analysis (VBA) is a whole-brain technique that allows regionally specific differences in brain tissue composition to be computed on a voxel-by-voxel basis. We performed statistical VBA analysis of the DTI and CHARMED maps by applying a repeated measures two-way analysis of variance (ANOVA) with 2 factors: before or after each learning session, and first week as oppose to the second week.

Statistical analysis was done on anatomical regions that were previously found by Sagi et al. (2012) in respect to our learning task. This includes the left hippocampus, bilateral parahippocampal gyrus and bilateral insular cortex. These regions were found to change structurally in a learning group, but not in control groups that did not participate in the task or in which spatial learning was attenuated (Sagi et al., 2012).

Results

Behavioral results

All subjects improved their performance in the task during the learning episode, as lap time decreased by 19 ± 2% (mean ± S.E.M., $p < 0.0001$) and their arrangement of the snapshots improved ($p < 0.0001$). The average lap time in each trial is shown in Fig. 1.

Changes in mean diffusivity

To compare with the results of the previous study we first wished to reexamine the effect of a 2 h spatial learning task on mean diffusivity. We performed a paired *t*-test on MD images of 23 subjects that were scanned before the learning procedure and immediately following the task. Statistical analysis was done on anatomical regions that were previously found by Sagi et al. (2012) in respect to our learning task. This includes the left hippocampus, bilateral parahippocampal gyrus and bilateral insular cortex. Voxels were considered significant for $P < 0.05$ (FDR corrected for multiple comparisons).

In accordance with the results of the previous study, significant clusters of MD reduction were found in all the regions of interest: in the anterior part of the left hippocampus (1.0 ± 0.3%, $P < 0.05$, corrected), in the bilateral posterior sections of the parahippocampal gyri (1.5 ± 0.3% and 1.2 ± 0.3% in the left and right hemispheres respectively, $P < 0.05$, corrected) and in the insular cortex of both hemispheres (1.5 ± 0.4% and 1.6 ± 0.4% in the left and right hemispheres respectively, $P < 0.05$, corrected). These results replicate the findings of our previous study (Sagi et al., 2012). The MD results are presented in Fig. 2, and values of MD reduction are shown in Fig. 3.

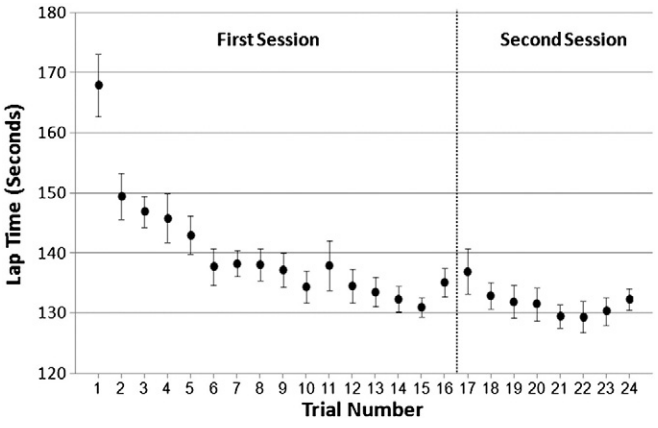

Fig. 1. Behavioral data. Performance in the car racing game is demonstrated by the average lap time of subjects in each trial. It is shown that most of the improvement was achieved during the early stages of the task, yet subtle decrease in lap time was observed in later trials as well. Error bars represents the standard error of the mean.

Time scale of changes

Besides the previously reported MD changes, the current study includes two additions: the use of the CHARMED protocol together with DTI, and a second series of scans a week after the first learning episode. In order to explore the dynamics of the structural brain changes we performed a voxel-based 2 (first\second week) × 2 (before\after learning) repeated measures analysis of variances (ANOVA) on the MD and Fr maps. This analysis was performed on the subset of 14 subjects that were scanned again a week after the first learning episode, on the same regions of interest. There were no significant MD effects (learning and week main effects, or interaction) using this analysis of only 14 subjects. While the MD changes extracted from DTI were too small and nonsignificant, the Fr maps showed a significant main effect of the learning procedure ($P < 0.05$, FDR corrected) in the left hippocampus, as the fraction of restricted component increased by 6.1 ± 2% after the first learning procedure, and by 2.7 ± 1% after the second learning procedure (Fig. 4). Between the two training sessions the Fr decreased by 3.2 ± 1%. A significant main effect of the learning procedure was also observed in the right parahippocampal gyrus ($P < 0.05$, FDR corrected), as the Fr increased by 2.6 ± 1% after the first learning procedure, and by 2.2 ± 1% after the second learning procedure (Fig. 5). Between the two training sessions the Fr barely changed (a decrease of 0.6 ± 1%). We didn't find any clusters of significant main effect for the learning procedure in any of the other regions of interest after correcting for multiple comparisons.

As expected, there was no significant main effect for the first \second week in any of the brain regions, meaning that there were no homogeneous differences between the scans of the first as opposed to the second week that are not related to the learning task. There was no interaction effect in any of the regions as well.

In addition, we examined whether there is any significant change in regions other than the *a-priori* defined ROIs and found no significant voxels for both MD and Fr maps outside the abovementioned ROIs when $P < 0.05$ (corrected for multiple comparisons).

Direct comparison between MD and Fr

In addition to the previously described analysis, we also wanted to compare the changes in MD and Fr directly. To do so, we performed a paired *t*-test between the relative change in MD to the relative change in Fr. The change in Fr was significantly bigger than the change in MD in the anterior hippocampus ($t = 2.3$, $P = 0.019$) and in the right PHG ($t = 1.88$, $P = 0.041$).

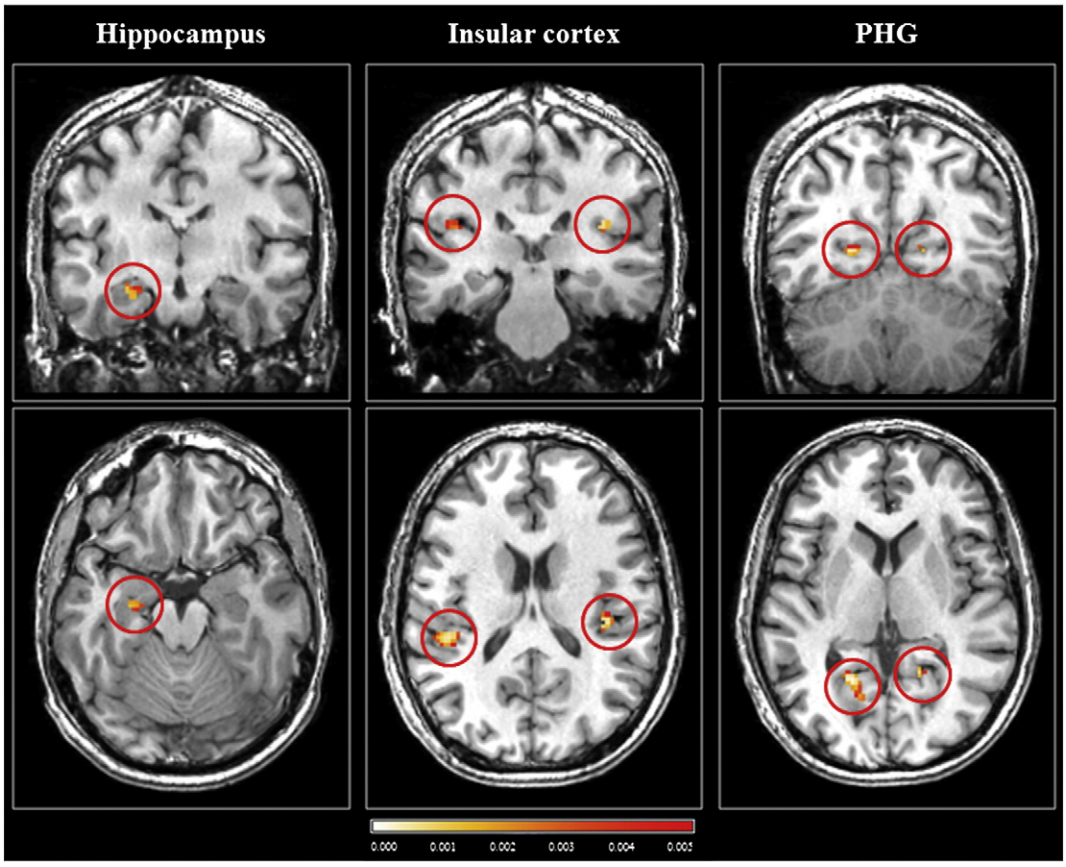

Fig. 2. Structural remodeling of brain tissue, measured by DTI as a reduction in mean diffusivity after 2 h of training on a spatial learning and memory task. *T*-test between the mean diffusivity (MD) maps before and after the learning task. The statistical parametric map is presented superimposed on coronal (upper row) and axial (lower row) slices of a single-subject T1 map. Voxels are considered significant when $p < 0.05$ (corrected for multiple comparisons). Significant clusters of MD decrease were found in the left hippocampus, insular cortex and parahippocampal gyrus (PHG) (marked in red circles).

Discussion

The current study provides further evidence of MR diffusion imaging ability to investigate short term neuroplasticity in humans. Changes in diffusion, that are indicative of structural changes in the tissue, were found using both DTI and CHARMED models after a short learning task. In particular, our results propose that the CHARMED framework is a sensitive method to detect structural plasticity that may provide better biological inference of these changes than the common DTI.

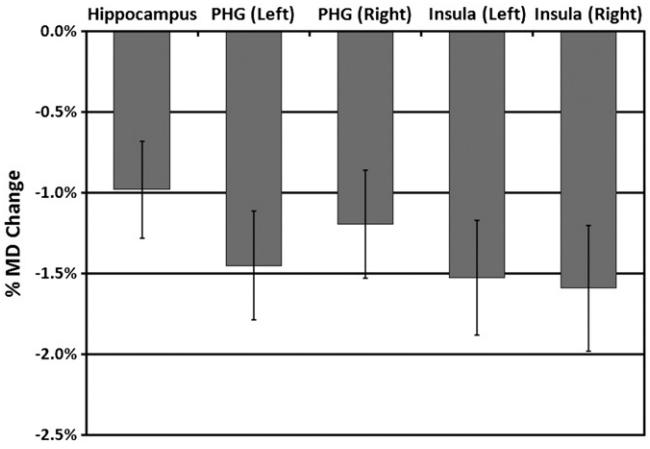

Fig. 3. Percentage of mean diffusivity (MD) reduction in clusters of significant change ($p < 0.05$, corrected). Error bars represent the standard error of the mean.

A previous study by Sagi et al. revealed a new time-scale of structural plasticity that can be measured *in-vivo* with DTI. A short spatial learning task of only 2 h yielded a decrease in MD indices, mainly in the left hippocampus and bilateral parahippocampal gyri. The current study provides additional support to these results with a new cohort of subjects that participated in the same task. A reduction of approximately 1.5% in mean diffusivity was found once more following 2 h of training in the anterior hippocampus, parahippocampal gyrus and insular cortex, known to be involved in spatial learning and memory.

Changes in diffusion following short learning were also found in the analysis of Fr maps, calculated from the CHARMED model. An increase in Fr was shown in the hippocampus and right parahippocampal gyrus. Moreover, the magnitude of change was more profound, seeing that Fr was increased by 6% as opposed to the decrement in MD (1.5%). This suggests that the CHARMED model is more sensitive to tissue's microstructure than DTI, and thus may depict more accurately the extent of the underlying changes in diffusion in the different tissue compartments.

The temporal dynamics of neuroplasticity

The sensitivity of CHARMED allowed to explore the progression of plasticity following two short learning sessions taken about one week apart. Significant changes in Fr in the hippocampus and parahippocampal gyrus were found both in the first 2 hour tryout and to a lesser extent in the shorter training that was completed after 6–8 days. DTI measurement failed to reveal such modifications. Furthermore, the observation

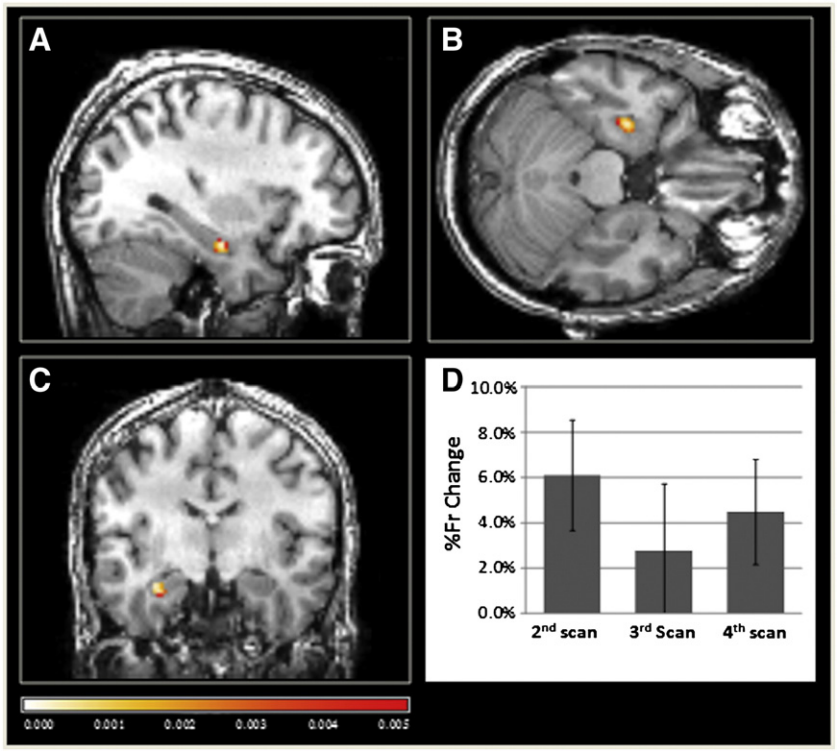

Fig. 4. Structural remodeling of brain tissue, measured by CHARMED as an increase in the volume fraction of restricted compartment (Fr). 2-Way repeated measures analysis of variance (ANOVA) on the Fr maps before and after the learning task, on the first and second week. The statistical parametric map is presented superimposed on sagittal (A), axial (B) and coronal (C) slices of a single-subject T1 map. Voxels are considered significant when $p < 0.05$ (corrected for multiple comparisons). A significant cluster of Fr increase is shown in the left hippocampus. The percentage Fr change in the hippocampal cluster relative to the first scan for each one of the scans is shown in (D).

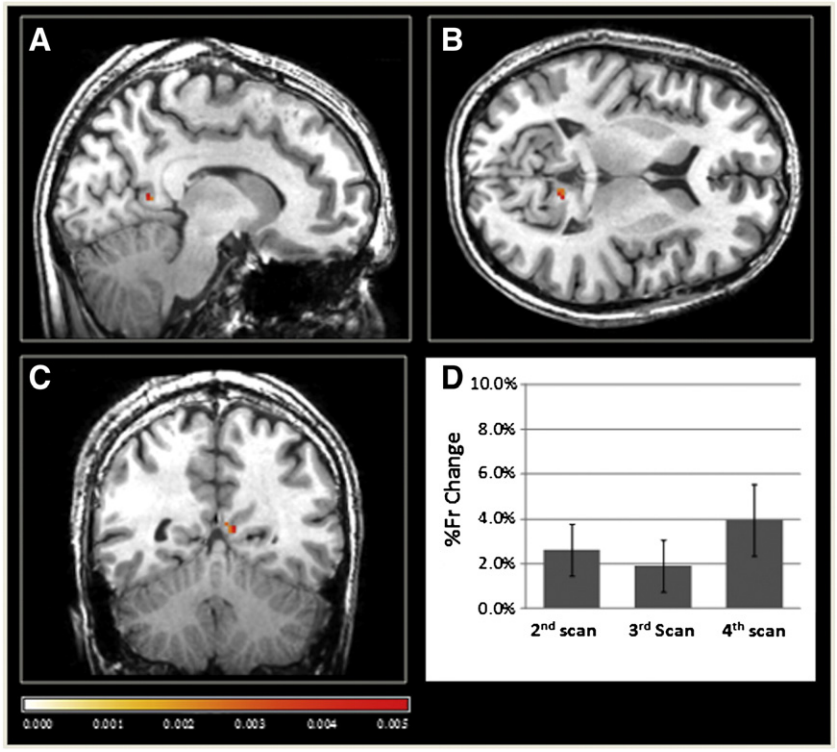

Fig. 5. Structural remodeling of brain tissue, measured by CHARMED as an increase in the volume fraction of restricted compartment (Fr). 2-Way repeated measures analysis of variance (ANOVA) on the Fr maps before and after the learning task, on the first and second week. The statistical parametric map is presented superimposed on sagittal (A), axial (B) and coronal (C) slices of a single-subject T1 map. Voxels are considered significant when $p < 0.05$ (corrected for multiple comparisons). A significant cluster of Fr increase is shown in the right parahippocampal gyrus. The percentage Fr change in the parahippocampal cluster relative to the first scan for each one of the scans is shown in (D).

that the remodeling re-occurred a week later and after a shorter training of only 45 min reflects the dynamics of structural reorganization that can reshape within minutes.

The relative return of Fr values to baseline a week after the first training task indicates that the structural changes that were measured immediately following the short learning session keep progressing (and probably influenced by other factors or tasks). The structural changes revealed in this study may indicate immediate remodeling of a network (probably at the glial level, see below) that is highly dynamic. Although not measured, it is reasonable to assume that events or tasks that happened following the learning episode weakened the measured changes, while strengthening other networks. Yet a support to the high dynamics of this phenomenon stems from the follow-up session that recreates a similar observation (probably due the formation of a similar network as in the first session) within minutes.

Biological interpretation of diffusion MRI changes

Although better defined in white matter, diffusion MRI is being used in recent years to investigate gray matter as well. The biological relevance of diffusion measures in gray matter is less straightforward: cells of different types and shapes, dendrites and other cellular processes that are randomly aligned causes diffusion indices to be less indicative of the underlying micro-structure. Even so, high resolution imaging of the gray matter indicates that the macroscopic arrangement of dendrites, axons and other cellular processes in gray matter are detectable with diffusion MRI (Jespersen et al., 2007). Moreover, a recent study even indicates that glial cell arrangement contributes to overall measured diffusion anisotropy (Budde et al., 2011). These observations, and others (Blumenfeld-Katzir et al., 2011; Darquié et al., 2001; Kroenke et al., 2005; Sasson et al., 2010), suggest that diffusion MRI analysis in gray matter is biologically meaningful.

DTI is sensitive to tissue's microstructure since the diffusion of water is affected by the geometry, viscosity and permeability of membranes within the tissue (Basser, 1995; Basser and Pierpaoli, 1996; Beaulieu, 2002). However, the calculated tensor is an average of all cellular components within the measured voxel, and does not provide comprehensive information on the different partitions that exist within the measured voxel. By modeling the hindered and restricted compartments the CHARMED framework offers a more complete exploration of the neural tissue, and as was shown here provides better sensitivity to the structural remodeling that develops in the tissue following new experiences. In addition, this separation to two partitions with different diffusion characteristics offers a more straightforward interpretation of the observed change in diffusion. Fr reflects the cylindrical organization and packing of the tissue as was shown in the white matter (Assaf and Basser, 2005). In white matter the assignment of Fr to axonal water was studied thoroughly (Assaf and Cohen, 2000). In gray matter the interpretation still needs experimental evidences however it can be assumed that Fr changes in the current study might be attributed to the remodeling of dendrite and glial processes. This interpretation is supported by two factors: 1. Dendrites and other neural processes have a cylindrical geometry that is modeled by Fr in CHARMED; 2. Dendrites and neural processes are known to change following plasticity. Astrocytes are vital partners in synaptic function, and exhibit rapid structural changes following synaptic activity (Theodosis et al., 2008). Their thin processes, which are 80% of the cell membrane (Lavialle et al., 2011), extract and retract in an activity dependent manner (Lavialle et al., 2011; Theodosis et al., 2008), and change their synapse coverage (Lushnikova et al., 2009). Evidence of structural plasticity in astrocyte morphology was previously shown in a study of rats that were trained in the Morris water maze (Blumenfeld-Katzir et al., 2011). Rats that learned the location of a platform showed a decrease in MD in several regions such as the dentate gyrus, as well as an increase in GFAP marker in an immuno-histological analysis and in the number of astrocyte processes. Rapid structural modifications have also been found in dendritic spines. The formation of dendritic spines after training was shown within an hour (Xu et al., 2009), inducing an increase in spine density (Hofer et al., 2009), and is associated with formation of new synapses. It is clear that more research is required in order to understand the basis of changes in diffusion and its biological correlates, but as proposed by Draganski and Kherif (2013) the use of MR imaging based on defined biophysical models can be a feasible *in-vivo* alternative to the difficulties in interpreting training dependent changes in MRI measurement in human studies.

Technical considerations

The results of the current study suggest that the CHARMED framework can be a valuable tool to investigate neuroplasticity. However, several issues should be taken into consideration. First, scanning time is relatively long, with the need to attain images at high b values in order to characterize the restricted compartment. In addition, low signal to noise ratio (SNR) in high b value images presents difficulties in motion correction and registration (Ben-Amitay et al., 2012). We used the approach suggested by Ben-Amitay et al. (2012) to deal with this issue. Low SNR also leads to problems in the optimization routine within the CHARMED model, causing many local maxima of the function. In the current study we overcome this problem by reducing the scan resolution and repeating the measurement (NEX = 2), both increasing the SNR but lengthening the scan time. In terms of applicability, advancements in gradient and radio-frequency technology will improve dramatically the use and reliability of this method. Lastly, the analysis process takes more time than DTI and requires more computational power. Nonetheless, by separating different tissue compartments and not averaging all parts of the tissue as in DTI, the CHARMED model can detect diverse structures within the measured voxel and better depict the modifications they undergo. This can be implemented in studies with smaller groups of subjects, and could help to detect regions that may not pass statistical analysis with conventional DTI measurements.

Another technical issue that should be considered is the timing of the experiments. In the current study design CHARMED was acquired first followed by DTI. This could potentially cause bias as the biological effects may differ between the two scans. However, in the previous study (Sagi et al., 2012) DTI was scanned immediately after the task. The results of the previous study were compared with those of the current one and did not differ significantly indicating that scanning time at the range of 20 min does not affect the observations. Future studies should include also randomization of the scanning ordering to remove this potential bias. In addition, the current study design was focused on the regional effects of the previous study (Sagi et al., 2012) that was performed including two control conditions. Future studies should aim to explore the Fr sensitivity also in the control groups.

Conclusions

We showed here that short term learning-induced structural brain changes are detectable using diffusion MRI. We suggest that the CHARMED framework characterizes the tissue microstructure more significantly and more sensitively than DTI and is therefore more suited to detect neuroplasticity in the micro-level. Using this method we were able to explore the dynamics of short term neuroplasticity and shed new light on this process. From our observations it appears that not only is the consolidation of a new skill in terms of structural plasticity rapid, but also its retrieval a week later.

Acknowledgments

The authors wish to thank the Israel Science Foundation (ISF grant 994/08), and the Future and Emerging Technologies (FET) Programme within the Seventh Framework Programme for Research of the European Commission (FET-Open, “CONNECT” project), grant 238292.

Conflict of interest

The authors have no conflict of interest to disclose.

References

Alexander, D.C., Hubbard, P.L., Hall, M.G., Moore, E.A., Ptito, M., Parker, G.J.M., Dyrby, T.B., 2010. Orientationally invariant indices of axon diameter and density from diffusion MRI. NeuroImage 52, 1374–1389.

Assaf, Y., Basser, P.J., 2005. Composite hindered and restricted model of diffusion (CHARMED) MR imaging of the human brain. NeuroImage 27, 48–58.

Assaf, Y., Cohen, Y., 2000. Assignment of the water slow-diffusing component in the central nervous system using q-space diffusion MRS: implications for fiber tract imaging. Magn. Reson. Med. 43, 191–199.

Assaf, Y., Pasternak, O., 2008. Diffusion tensor imaging (DTI)-based white matter mapping in brain research: a review. J. Mol. Neurosci. 34, 51–61.

Assaf, Y., Freidlin, R.Z., Rohde, G.K., Basser, P.J., 2004. New modeling and experimental framework to characterize hindered and restricted water diffusion in brain white matter. Magn. Reson. Med. 52, 965–978.

Barazany, D., Basser, P.J., Assaf, Y., 2009. *In vivo* measurement of axon diameter distribution in the corpus callosum of rat brain. Brain 132, 1210–1220.

Basser, P.J., 1995. Inferring microstructural features and the physiological state of tissues from diffusion-weighted images. NMR Biomed. 8, 333–344.

Basser, P.J., Pierpaoli, C., 1996. Microstructural and physiological features of tissues elucidated by quantitative-diffusion-tensor MRI. J. Magn. Reson. B 111, 209–219.

Beaulieu, C., 2002. The basis of anisotropic water diffusion in the nervous system—a technical review. NMR Biomed. 15, 435–455.

Ben-Amitay, S., Jones, D.K., Assaf, Y., 2012. Motion correction and registration of high b-value diffusion weighted images. Magn. Reson. Med. 67, 1694–1702.

Bezzola, L., Mérillat, S., Gaser, C., Jäncke, L., 2011. Training-induced neural plasticity in golf novices. J. Neurosci. 31, 12444–12448.

Blumenfeld-Katzir, T., Pasternak, O., Dagan, M., Assaf, Y., 2011. Diffusion MRI of structural brain plasticity induced by a learning and memory task. PLoS One 6, e20678.

Bruel-Jungerman, E., Davis, S., Laroche, S., 2007. Brain plasticity mechanisms and memory: a party of four. Neuroscientist 13, 492–505.

Bruel-Jungerman, E., Rampon, C., Laroche, S., 2007. Adult hippocampal neurogenesis, synaptic plasticity and memory: facts and hypotheses. Rev. Neurosci. 18, 93–114.

Budde, M.D., Janes, L., Gold, E., Turtzo, L.C., Frank, J.A., 2011. The contribution of gliosis to diffusion tensor anisotropy and tractography following traumatic brain injury: validation in the rat using Fourier analysis of stained tissue sections. Brain 134, 2248–2260.

Darquié, A., Poline, J.B., Poupon, C., Saint-Jalmes, H., Le Bihan, D., 2001. Transient decrease in water diffusion observed in human occipital cortex during visual stimulation. Proc. Natl. Acad. Sci. U. S. A. 98, 9391–9395.

Draganski, B., Kherif, F., 2013. In vivo assessment of use-dependent brain plasticity - beyond the "one trick pony" imaging strategy. NeuroImage 73, 255–259 discussion 265–267.

Draganski, B., Gaser, C., Busch, V., Schuierer, G., Bogdahn, U., May, A., 2004. Neuroplasticity: changes in grey matter induced by training. Nature 427, 311–312.

Galván, A., 2010. Neural plasticity of development and learning. Hum. Brain Mapp. 31, 879–890.

Hofer, S.B., Mrsic-Flogel, T.D., Bonhoeffer, T., Hübener, M., 2009. Experience leaves a lasting structural trace in cortical circuits. Nature 457, 313–317.

Holtmaat, A., Svoboda, K., 2009. Experience-dependent structural synaptic plasticity in the mammalian brain. Nat. Rev. Neurosci. 10, 647–658.

Jespersen, S.N., Kroenke, C.D., Østergaard, L., Ackerman, J.J.H., Yablonskiy, D.A., 2007. Modeling dendrite density from magnetic resonance diffusion measurements. NeuroImage 34, 1473–1486.

Johnston, M.V., 2009. Plasticity in the developing brain: implications for rehabilitation. Dev. Disabil. Res. Rev. 15, 94–101.

Kroenke, C.D., Bretthorst, G.L., Inder, T.E., Neil, J.J., 2005. Diffusion MR imaging characteristics of the developing primate brain. NeuroImage 25, 1205–1213.

Lavialle, M., Aumann, G., Anlauf, E., Pröls, F., Arpin, M., Derouiche, A., 2011. Structural plasticity of perisynaptic astrocyte processes involves ezrin and metabotropic glutamate receptors. Proc. Natl. Acad. Sci. U. S. A. 108, 12915–12919.

Lushnikova, I., Skibo, G., Muller, D., Nikonenko, I., 2009. Synaptic potentiation induces increased glial coverage of excitatory synapses in CA1 hippocampus. Hippocampus 19, 753–762.

Maguire, E.A., Gadian, D.G., Johnsrude, I.S., Good, C.D., Ashburner, J., Frackowiak, R.S., Frith, C.D., 2000. Navigation-related structural change in the hippocampi of taxi drivers. Proc. Natl. Acad. Sci. U. S. A. 97, 4398–4403.

Münte, T.F., Altenmüller, E., Jäncke, L., 2002. The musician's brain as a model of neuroplasticity. Nat. Rev. Neurosci. 3, 473–478.

Sagi, Y., Tavor, I., Hofstetter, S., Tzur-Moryosef, S., Blumenfeld-Katzir, T., Assaf, Y., 2012. Learning in the fast lane: new insights into neuroplasticity. Neuron 73, 1195–1203.

Sasson, E., Doniger, G.M., Pasternak, O., Assaf, Y., 2010. Structural correlates of memory performance with diffusion tensor imaging. NeuroImage 50, 1231–1242.

Scholz, J., Klein, M.C., Behrens, T.E.J., Johansen-Berg, H., 2009. Training induces changes in white-matter architecture. Nat. Neurosci. 12, 1370–1371.

Theodosis, D.T., Poulain, D.A., Oliet, S.H.R., 2008. Activity-dependent structural and functional plasticity of astrocyte–neuron interactions. Physiol. Rev. 88, 983–1008.

Tuch, D.S., Reese, T.G., Wiegell, M.R., Makris, N., Belliveau, J.W., Wedeen, V.J., 2002. High angular resolution diffusion imaging reveals intravoxel white matter fiber heterogeneity. Magn. Reson. Med. 48, 577–582.

Xu, T., Yu, X., Perlik, A.J., Tobin, W.F., Zweig, J.A., Tennant, K., Jones, T., Zuo, Y., 2009. Rapid formation and selective stabilization of synapses for enduring motor memories. Nature 462, 915–919.